Breast Symmetry Classification: A Proposal of Image Analysis Based Indices

Eudóxia L. S. Moura
Federal Institute of Rondônia
Ariquemes, Rondônia, Brazil
eudoxia.moura@ifro.edu.br

Flávia C. H. Pastura
Natascha Scagliusi
Wanessa I. Oliveira
Industrial Design Division of National Institute of Technology
Rio de Janeiro, Rio de Janeiro, Brazil

Aura Conci
Computer Institute, Fluminense Federal University
Niterói, Rio de Janeiro, Brazil
aconci@ic.uff.br

Abstract

The study aims to develop a method for evaluating breast symmetry using profile images. This shape-based analysis assesses differences between the two profiles with the help of simple indices, enabling an external symmetry evaluation independent of the image acquisition method. Initially, thermograms of 62 volunteers were analyzed, leading to the proposal of four asymmetry indices based on measurements of breast profile. Subsequently, images from 30 additional volunteers were examined to determine whether a multimodal pattern emerged across different imaging techniques, including infrared (IR) cameras, three-dimensional (3D) scan models, and photographic (RGB) cameras. To validate the method and assess the feasibility of applying the proposed indices to these imaging methods, the classified images (as symmetric or asymmetric) were evaluated by 28 specialists. The comparison between the proposed indices and expert assessments resulted in an accuracy rate of 60%.

CCS Concepts

• **Computing methodologies** → **Computer vision tasks**; • **Applied computing** → **Health care information systems**.

Keywords

thermography, breast cancer, breast asymmetry

How to cite this paper:
Eudóxia L. S. Moura, Flávia C. H. Pastura, Natascha Scagliusi, Wanessa I. Oliveira, and Aura Conci. 2025. Breast Symmetry Classification: A Proposal of Image Analysis Based Indices. In *Proceedings of ACM IMX Workshops, June 3 - 6, 2025*. SBC, Porto Alegre/RS, Brazil, 6 pages.
https://doi.org/10.5753/imxw.2025.5735

1 Introduction

Beyond its biological role in breastfeeding, the breast also contributes to aesthetics and self-confidence. This is evident from the fact that breast augmentation surgery is the second most common plastic surgery worldwide [12]. In many countries, women have undergone plastic surgery through public health systems [2]. In Brazil alone, 1,474 breast reconstructive surgeries after mastectomy were performed by SUS in 2023 [3].

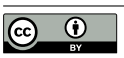

Like many other parts of the human body, breasts naturally exhibit counter-symmetry along the cranio-caudal axis. Under normal conditions, the right and left breasts can be considered mirrored images; however, this symmetry is not exact, much like other human body structures and natural forms. For instance, the right hand is not an exact replica of the left when inverted and superimposed. The same applies to arms, legs, and even internal organs such as the kidneys and lungs.

However, significant asymmetry - whether external or internal - is not considered natural. In breast examinations, pronounced differences are often key indicators of potential abnormalities. This concept is illustrated in Figure 1, which compares mammography, magnetic resonance imaging (MRI), and thermography of the right and left breasts in a patient with unilateral lobular carcinoma near the nipple region [7].

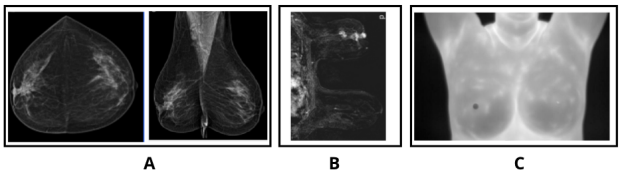

Figure 1: (A) Craniocaudal (CC) and mediolateral oblique (MLO) views of the right and left breasts captured through mammography, (B) magnetic resonance imaging (MRI), and (C) infrared (IR) thermography [7].

Examining the three imaging modalities in Figure 1, a lack of internal symmetry is evident across all of them. Additionally, when observing the boundary between the patient's skin and the black background in the first three imaging types, this asymmetry is also externally apparent. This indicates that the internal asymmetry caused by the retraction of mammary tissue due to carcinoma affects the breast's visible surface.

While this is an advanced case, similar asymmetries can also be observed during early screening. Asymmetry should be assessed at different evolutive levels, but accurately quantifying the "degree of asymmetry" in early detection is challenging. For this reason, diagnostic reports from various imaging exams often require the evaluation of at least three radiologists. This applies to both anatomical exams, such as mammography and non-contrast MRI, as well as physiological exams, including ultrasound, thermography, and contrast-enhanced MRI.

Thermography is perhaps the least known imaging method for cancer diagnosis. It utilizes infrared cameras to capture thermal images of the body surface, detecting temperature anomalies that may indicate the presence of tumors [6, 11, 19]. However, this method is prone to false positives, requiring more sophisticated symmetry analyses beyond simple statistical approaches to improve diagnostic accuracy and minimize unnecessary alarm [18].

As a physiological imaging technique, thermography has gained interest due to its non-invasive nature — it does not require physical contact or external agents to acquire data, relying solely on the natural infrared radiation emitted by molecular activity. It is suitable for women at any stage of life, including during pregnancy, with costs limited to the acquisition of appropriate infrared cameras and the expertise of a specialist or intelligent image analysis systems for interpretation. Additionally, thermography can be used for postoperative monitoring or as a presurgical tool in adjuvant treatment following a malignant diagnosis confirmed by biopsy [1].

The breast is an organ present in both sexes and remains identical in males and females until puberty. Changes in its external shape are often visible without medical equipment and can help identify certain rare pathologies, such as Paget's disease. This type of cancer affects the nipple and areola, with tumor cells typically spreading through the mammary ducts. Diagnosis is clinical and confirmed through a skin biopsy, and with proper treatment, the cure rate exceeds 95% [16].

Scientific literature highlights the importance of anthropometric features — such as body mass index (BMI), waist circumference, and waist-hip ratio — to understand different stages of cancer development. A recent study found that specific body silhouette traits may indicate hormonal imbalances in women with breast cancer [17]. These findings emphasize the importance of diagnostic methods that consider anatomical variability, enabling a more accurate assessment of symmetry across various body types.

Another application of symmetry evaluation is in cosmetic and reconstructive breast surgeries. A simple and efficient method that plastic surgeons can use in their offices — or even one that individuals can utilize with a smartphone camera — would be highly valuable in assessing the success of reconstructions or determining the necessary volume for silicone implants.

This study aims to propose simple measurement methods and quantitative evaluations for assessing breast symmetry (or asymmetry). These methods were initially formulated based on infrared (IR) images of 62 patients from the Academic Hospital, using a static acquisition protocol capturing images from five different angles (0º, 45º, 90º, 135º and 180º). The protocol, which acquire data in the infrared frequency range, was approved by the Hospital's Ethics Committee and registered with the Brazilian Ministry of Health under CAAE number 01042812.0.0000.5243 [20].

To further validate these methods, additional imaging was performed using different modalities with new volunteers. For this phase, 30 women consented to have their breasts form captured using 3D scanning and IR thermography. Each volunteer provided informed consent for the use of their data and images. Among them, 20 also had their images captured in visible light frequencies, allowing a comparative analysis between infrared imaging and RGB digital photography, similar to those used in contemporary smartphone cameras.

2 Related works on external symmetry

The first software developed for aesthetic evaluation of patients undergoing cosmetic surgery after breast cancer treatment was the Breast Cancer Conservative Treatment Cosmetic Result (BCCT.core), introduced in 2007. BCCT.core provided an objective method for assessing breast aesthetics using a classifier based on Support Vector Machine (SVM). This software analyzed a two-dimensional (2D) frontal image, as shown in the schematic diagram in Figure 2A. It classified outcomes into four categories: excellent, good, fair, and poor. These categories were created based on clinical observations to support surgical planning and guide the treatment of breast asymmetries. The evaluation considered factors such as breast volume, breast asymmetry, skin color differences, and scar visibility.

According to the authors, BCCT.core achieved a 70% correct classification rate [4]. However, these results were not established by verifiable and comparable measurements. The software calculates breast asymmetry and volume using several indices, including: the difference in nipple position between the breasts (Breast Retraction Assessment or BRA), the difference in the lower breast contour level (Lower Breast Contour or LBC), the difference in nipple heights (Upward Nipple Retraction or UNR), the difference in the distance from the left and right nipples to the inframammary fold (Breast Compliance Evaluation or BCE), the difference in the lengths of the breast contours (Breast Contour Difference or BCD), the difference in breast areas (Breast Area Difference or BAD), and the difference between one breast overlaid onto the other after mirroring along a vertical axis and aligning the two junction points with the thorax (Breast Overlap Difference or BOD) [5].

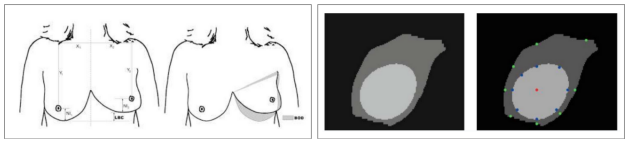

Figure 2: (A) Sketch with some of the measurements used in BCCT.core [4]; (B) Depth map displaying 3 levels and reference points [10] .

In 2016, a new method for analyzing the three-dimensional (3D) shape of the breast was introduced. This technique involves acquiring 3D breast surface data, aligning and projecting these surfaces into a 2D plane, segmenting the region of interest (ROI) based on anatomical points derived from a set of 17 geometric landmarks, and validating the results using Principal Component Analysis (PCA) [10]. To capture the 3D breast surfaces, a low-cost portable scanner utilizing structured infrared light is used to generate a depth map of the scanned area. Automatic alignment of the breast model is achieved by following the normal orientations of the surface [10]. The segmentation of the ROI is performed based on four anatomical points suggested by specialists, and the breasts are mirrored vertically to standardize the dataset for both the right and left sides [10]. The 17 reference points are extracted as follows: the first reference point is the highest original depth value, which may or may not correspond to the nipple, and is marked in red in Figure 2B (right side).

The second set of eight reference points is determined by identifying the intersections of lines extending from the first point in eight fixed directions, each separated by a 45º angle (i.e., 0º, 45º, ..., 315º), and the boundary of the highest quantization level, is depicted in blue in Figure 2BB. The final eight landmarks are then selected using the same strategy but based on the second quantization level. Principal Component Analysis (PCA) is subsequently applied, reducing the number of components so that each breast can be represented by two coordinates (x and y) of a minimal set of points. A mastologist reviewed these points and concluded that the principal component along the x-axis is not particularly significant, whereas the y-axis component effectively captures breast size and ptosis variability [10].

In 2017, a digital application was developed to detect and assess breast symmetry. This method operates on the fundamental assumption that the lower part of the breasts resembles arcs of circles. In the initial stage of the process, the Hough Transform (HT) image analysis technique is employed to identify circular shapes within the image. The application then compares the radii of these detected circles to evaluate breast symmetry, as illustrated in Figure 3. The asymmetry percentage is determined by averaging the sum of these values [15].

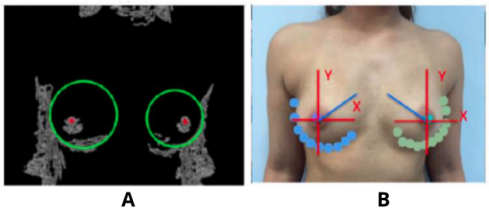

Figure 3: (A) Detection of circles using the Hough Transform; (B) Measurement of distances from the nipple to the circumferences, defining various possible radii for breast comparison [15].

3 Materials and Methods

A total of 30 volunteers participated in this study, providing both thermographic images and 3D scans. Among them, 21 volunteers also provided images captured in the visible spectrum using a standard digital RGB camera. All image acquisitions were conducted at the same time and location, specifically at the Industrial Design Division of the National Institute of Technology (INT). Each participant signed an informed consent form (ICF) agreeing to take part in the research.

The acquisition process followed a protocol approved and registered with the Ministry of Health (01042812.0.0000.5243 [20]. Thermographic images were captured using a Hikmicro SP60H thermographic camera, which features a thermal resolution of 640×480 pixels (307,200 thermal pixels) and a thermal contrast or Noise Equivalent Temperature Difference (NETD) of $0.03°C$ (or 30×10^{-3} degrees Kelvin). The room temperature during image acquisition ranged from $22.1°C$ to $24.6°C$. The lens used had a horizontal field of view of 24.8° and a vertical field of view of 18.7°, with all images stored in Portable Network Graphics (PNG) format.

For each participant, five images were captured from different angles relative to the body's frontal axis: 0°, 45°, 90°, -45°, and -90°, as illustrated in Figure 4.

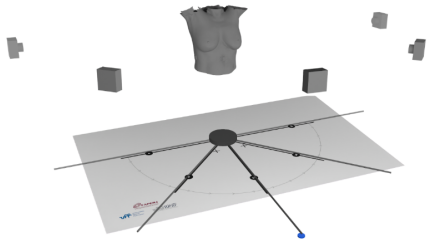

Figure 4: Camera capture angles used in this study

The three-dimensional scanning of the 30 volunteers was performed using an Artec 3D Leo portable structured white light scanner. The scanning process began on the right side of the body and progressed to the left, focusing on the regions of interest, specifically from the breasts to the armpits. Artec Studio 18 software was utilized, with HD mode for scanning and fast mode for surface merging. This configuration, recommended by the manufacturer for measurement applications, ensured the reliability of the collected data. No scanning failures were observed, and there were no occluded points or noise requiring removal. As a result, all original scanned shapes and details were fully preserved. The final 3D models were saved in Polygon File Format (PLY), generating the 3D images shown in the center of Figure 4.

In thermographic imaging, two primary protocols are used: static and dynamic [20]. Static protocols involve capturing thermal images at five different angles while the patient remains in thermal equilibrium with the environment (static acquisitions). Dynamic protocols, in contrast, require a series of captures following an artificial change in body surface temperature until thermal equilibrium is restored (dynamic acquisitions) [9]. In this study, only images obtained using the static protocol were utilized, with the camera positioned orthogonally to the body's frontal axis. These breast profile captures are illustrated in Figure 5.

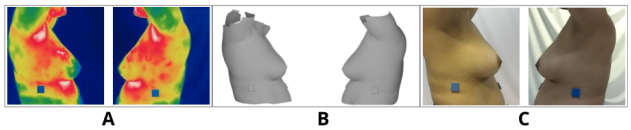

Figure 5: Profile images of a volunteers' breasts: (A) Infrared (IR) or thermographic image; (B) 3D scan image, and (C) RGB or visible spectrum image.

High-temperature regions are often found in areas of the body with limited ventilation, leading to reduced heat exchange with the environment. Common examples include the armpits and the inframammary fold (the area beneath the breasts). However, elevated temperatures may also indicate increased vascular activity, inflammation, or internal heat caused by the proliferation of cancerous

cells spreading through breast tissues to the surface (an underlying principle of thermography in medical diagnostics) [13].

The first two images in Figure 5 display infrared (IR) scans using a false-color palette, where deep blue represents the ambient temperature, while yellow, red, and white indicate progressively warmer body regions.

3.1 Points for assessment

The proposed evaluation method consists of four stages. The first stage, ROI segmentation, involves isolating the breast region from the rest of the frame captured by the camera. In the second stage, point detection, specific anatomical points are identified for the analysis. The third stage, parameter calculation, includes measuring various parameters such as linear distances and areas. The final stage, comparison and calculation, evaluates absolute and relative differences in these measurements, comparing them to breast models classified by a panel of 28 experts as symmetric, asymmetric, or undefined.

Although the static acquisition protocol captures images from five different angles, this study focuses solely on lateral images. These side-view images provide clear profiles of the left and right breasts, enabling the identification of key points for symmetry evaluation. In the left lateral images, the analyzed points are labeled with the letter "L," while those in the right lateral images are marked with "R." The points representing the nipples on each side are indicated by the letter "N," defined as the farthest point horizontally to the right or left in the image.

Another key point is the lowest part of the inframammary fold, labeled as "I." In right and left lateral images, these points are mirrored along a vertical axis. The inframammary fold is represented as RI (right inframammary) and LI (left inframammary), while the nipples are marked as RN (right nipple) and LN (left nipple). Linear distances from inframammary points to the nipples points are used for analysis. Figure 6 illustrates these key points on each breast. This analysis is applied across all profile images, regardless of the acquisition technique, whether in the visible spectrum (RGB), thermal imaging, or three-dimensional scanning.

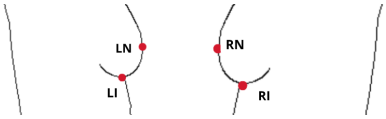

Figure 6: Evaluation points: LN (left nipple), LI (left inframammary), RN (right nipple), and RI (right inframammary).

3.2 Calculations of distances and areas

By identifying the evaluation points, linear distances in pixels can be calculated for all images. For the right breast, the measured distances include Euclidean (ER), horizontal (HR), and vertical (VR), while the corresponding measurements for the left breast are Euclidean (EL), horizontal (HL), and vertical (VL).

Using these predefined points and computed linear measurements, each breast can be approximated by an ellipse (see Figure 7). The HR and VR measurements define the ellipse in the right lateral view (RA), while the HL and VL measurements are used for the left lateral view (LA). The fitted ellipses for each breast are then compared based on their surface differences (area). This comparison involves analyzing the overlap between ellipses obtained from infrared (IR) imaging and those from the 3D scanner.

For each volunteer, three linear measurements and one area measurement are considered. The differences between the right and left breasts are then calculated based on these measurements. For example, the vertical difference is determined as: | **VR** - **VL** |.

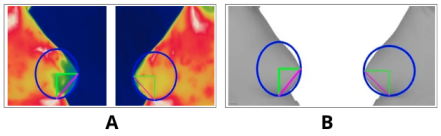

Figure 7: Elliptical approximation of each breast: (A) thermal image; (B) 3D scan model.

These measurements are calculated in pixels, but a higher pixel count from one volunteer to another does not necessarily indicate greater breast asymmetry, as the distance from the camera can vary between volunteers. To account for this, square thermal insulating stickers were affixed to the participants' bodies. These stickers, made of ethylene vinyl acetate (EVA), have a thickness of 2 mm and a side length of 1 inch (25.4 millimeters). They were placed on both the lateral and frontal views of the volunteers. If the square appears smaller in the image, it indicates that the participant is farther from the camera; if it appears larger, the participant is closer. This effect is illustrated in Figure 8, where the volunteer on the right is positioned closer to the camera than the one on the left. Based on these reference stickers, four scale measurements are obtained: area scale (as), vertical scale (vs), horizontal scale (hs), and Euclidean scale (es).

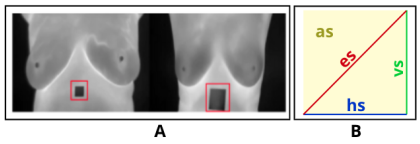

Figure 8: (A)Examples of EVA square stickers and the four derived scale measurements: area scale (as), vertical scale (vs), horizontal scale (hs), and Euclidean scale (es).

To ensure independence from the distance between the patient and the camera, the asymmetry index is calculated using the following formula:

Asymmetry Index = {Difference / Scale}

Difference represents the measurement of the right breast minus the corresponding measurement of the left breast, and **Scale** refers to the measurement of the reference square. This approach eliminates the impact of camera distance, allowing for a consistent comparison of breast symmetry.

The proposed asymmetry indices include the horizontal distance index (iH), which quantifies differences in breast positioning along

Table 1: Calculated Asymmetry Indices: Classification in Red (Asymmetric) and Green (Symmetric) .

	IR				3D				RGB			
Volunteer	**ir_*iV***	**ir_*iH***	**ir_*iE***	**ir_*iA***	**sc_*iV***	**sc_*iH***	**sc_*iE***	**sc_*iA***	**rgb_*iV***	**rgb_*iH***	**rgb_*iE***	**rgb_*iA***
M001	0.3	0.6	0.3	0.2	0.3	0.3	0.3	8.9	-	-	-	-
M002	0.3	0.1	0.2	2.5	0.4	0.1	0.2	2.1	-	-	-	-
M003	0.1	0.0	0.1	1.0	0.2	0.0	0.1	1.7	0.3	0.2	0.3	5.3
M004	0.1	0.0	0.0	0.2	0.2	0.2	0.0	0.0	0.2	0.2	0.2	5.2
M005	1.4	1.5	1.4	27.7	1.0	0.8	0.9	21.0	0.7	0.5	0.2	1.8
M006	0.2	0.5	0.1	5.4	0.4	0.6	0.0	3.1	0.0	0.9	0.3	11.8
M007	0.2	0.2	0.0	0.5	0.0	0.2	0.1	3.7	0.6	0.6	0.6	16.4
M008	0.2	0.2	0.0	0.9	0.0	0.7	0.3	7.4	0.3	0.1	0.2	3.5
M009	0.1	0.2	0.1	4.9	0.2	0.1	0.0	0.6	0.2	0.7	0.4	12.6
M010	0.0	0.4	0.1	5.5	0.0	0.3	0.2	5.0	-	-	-	-
M011	0.1	0.4	0.3	6.5	0.2	0.5	0.4	9.8	0.7	0.9	0.8	18.4
M012	0.1	0.1	0.0	0.6	0.2	0.0	0.1	1.9	0.1	0.0	0.1	1.3
M013	0.2	0.2	0.0	1.2	0.2	0.4	0.3	7.6	0.4	0.3	0.3	7.8
M014	0.2	0.2	0.2	4.4	0.0	0.3	0.1	3.8	0.2	0.1	0.2	3.3
M015	0.0	0.2	0.1	3.0	0.0	0.3	0.2	7.2	0.0	0.3	0.2	5.6
M016	0.2	0.1	0.1	0.1	0.2	0.2	0.1	1.2	0.3	0.4	0.3	11.5
M017	0.2	0.3	0.0	3.4	0.1	0.1	0.0	1.1	0.3	0.1	0.2	3.9
M018	0.0	0.2	0.1	2.7	0.2	0.0	0.1	1.3	0.0	0.3	0.1	4.2
M019	0.7	0.8	0.7	13.1	0.1	0.2	0.2	3.7	0.8	1.4	1.1	23.3
M020	0.1	0.7	0.3	9.9	0.3	0.4	0.3	10.1	0.1	0.6	0.1	9.1
M021	0.1	0.1	0.1	3.0	0.2	0.1	0.1	2.2	0.6	0.5	0.5	15.5
M022	0.3	0.2	0.3	6.0	0.2	0.3	0.1	1.3	0.3	0.6	0.4	9.6
M023	0.3	0.0	0.1	3.8	0.0	0.2	0.1	4.2	0.0	0.9	0.4	14.1
M024	0.1	0.1	0.1	2.5	0.1	0.0	0.0	0.6	0.1	0.5	0.2	6.7
M025	0.1	0.0	0.0	0.6	0.2	0.2	0.0	1.2	-	-	-	-
M026	0.2	0.2	0.2	4.7	0.0	0.1	0.1	2.0	-	-	-	-
M027	0.5	0.5	0.5	12.9	0.5	0.0	0.3	9.1	-	-	-	-
M028	0.2	0.5	0.3	9.3	0.1	0.4	0.2	7.0	-	-	-	-
M029	0.3	0.6	0.4	11.7	0.3	0.3	0.3	8.8	-	-	-	-
M030	0.7	0.1	0.4	10.9	0.4	0.1	0.3	7.8	-	-	-	-

the horizontal axis, the vertical distance index (iV), which evaluates variations in height, the Euclidean distance index (iE), which considers the total distance between the nipple and the inframammary fold, and the area index (iA), which assesses differences in the fitted ellipses representing each breast.

From the DMI database ([20]), a total of 34 volunteers were evaluated in Moura's (2024) study, with initial segmentation performed in Costa's (2020) research. Breast classification into symmetrical (S), asymmetrical (A), or doubtful (D) categories was validated by 28 breast thermography specialists. These experts completed a questionnaire, assigning left and right breast images to one of the three categories.

After classified, images were then compared to numerical indices. A volunteer was classified as symmetrical (S) if over 75% of evaluators identified her as such, as asymmetrical (A) if more than 75% classified her that way, and as doubtful (D) if neither classification applied. Among the 34 volunteers, 9 were classified as symmetrical, 6 as asymmetrical, and 19 remained in the doubtful category.

Based on these results, a quantitative criterion was proposed: breasts are considered asymmetrical if the values of the linear indices ((iH), (iV), (iE)) are greater than 0.8 and symmetrical if they are lower than 0.2. For the area index (iA), values above 4.0 indicate asymmetry, while values below 0.3 indicate symmetry [14].

4 Results

The results obtained by computing the four proposed measures are presented in Table 1 across the three acquisition modes: thermography (IR), 3D scan model, and RGB (visible spectrum) imaging. In the table, red and green cell highlights indicate when an index classifies a patient as asymmetric or symmetric, respectively.

Regarding the classification of symmetry, applying the same classification threshold to the 30 new volunteers allows us to conclude that:

(1) The three linear indices successfully identified volunteers with symmetrical breasts in both infrared (IR) and scan images. In the IR images, 12 volunteers (M003, M004, M007, M009, M012, M015, M016, M018, M021, M024, M025, and M026) were classified as symmetrical. In the 3D scan model images, only 8 volunteers (M003, M009, M012, M017, M018, M024, M025, and M026) maintained this classification. Comparing both methods, the classification was consistent for 7 volunteers. When considering the area index, only three volunteers (M001, M004, and M016) were classified as symmetrical in the IR images, with only M004 maintaining this classification in the 3D scan model images.

(2) In the analysis of RGB images, volunteers classified as symmetrical based on linear measurements were M012 and M014, while the area-based index did not classify any volunteer as symmetrical. To validate the method, 10 specialists conducted a subjective evaluation of volunteers M003, M005, M011, M012, M018, M020, M024, M025, M026, M029, and M030. Among them, M005, M018, and M026 were considered asymmetrical by more than 60% of the evaluators, whereas M003, M011, M025, and M029 were classified as symmetrical by the same percentage of specialists.

(3) Regarding asymmetry classification, only volunteer M005 was identified as asymmetrical based on linear measurements in both infrared (IR) and 3D scan model images. When considering area-based measurements, the IR image analysis classified the following

volunteers as asymmetrical: M005, M006, M009, M010, M011, M014, M019, M020, M022, M026, M027, M028, M029, and M030. In the 3D scan model images, the volunteers classified as asymmetrical were M001, M005, M008, M010, M011, M013, M015, M020, M023, M027, M028, M029, and M030. A comparison of both methods showed that the classification was consistent for 8 volunteers. In the RGB images, 16 volunteers were classified as having asymmetrical breasts: M003, M004, M006, M007, M009, M011, M013, M015, M016, M018, M019, M020, M021, M022, M023, and M024.

5 Conclusion

This study supports the use of three linear classification indices for assessing breast symmetry in infrared (IR) images. Similar properties were observed in 3D scan images, though further research is needed to extend these findings to images in the visible spectrum, such as RGB. For asymmetry evaluation, additional studies are necessary, particularly focusing on women with breast conditions, as most volunteers in this study had no diagnosed breast diseases.

Simple indices were proposed to evaluate breast symmetry, and despite method's simplicity, the results closely align with previous studies analyzing the effects of conservative breast cancer surgery [4]. The proposed method offers a quantitative approach to breast evaluation and can serve as an indicator of breast shape, using images captured by thermographic or conventional cameras, as the results obtained in RGB images were equivalent to those of thermographic images.

Future research should further investigate RGB images and 3D scanning models in order to establish more precise thresholds for different imaging techniques. The investigation of automatic segmentation methods, as well as the refinement of these methods and the definition of new evaluation points, may increase analysis accuracy, especially for images captured from different angles. Moreover, it is recommended to carry out a more robust statistical analysis of the correlation between the proposed indices and expert evaluations. It is also important to discuss potential practical implementations in mobile device applications, as well as to address in more detail the clinical implications of the proposed indices and how they could be integrated into medical assessment workflows.

6 Acknowledgments

We would like to thank the 30 volunteers who signed the consent form, authorizing the use of their data and images. A special thanks to the 20 who allowed measurements on images in the visible spectrum, enabling comparisons between infrared and RGB images from digital cameras and smartphones.

E.L.S.M. is supported by Federal Institute of Education, Science and Technology of Rondônia (IFRO). A.C. is supported in part by the National Institutes of Science and Technology (INCT - MACC project), National Council for Scientific and Technological (CNPq) under grant 307638/2022-79, the Research Support Foundation of Rio de Janeiro State (FAPERJ) over CNE, e-Health Rio and Digit3D ("temáticos") projects [8].

References

[1] A. S. Araújo, M. H. S. Issa, Á. Sánchez, D. C. Muchaluat-Saade, and A. Conci. 2023. Termografia como Ferramenta de Avaliação Durante o Tratamento Neoadjuvante para Câncer de Mama. In *Simpósio Brasileiro de Computação Aplicada à Saúde (SBCAS), 23.* Sociedade Brasileira de Computação, São Paulo/SP, 280–291. doi:10.5753/sbcas.2023.229813

[2] Brasil. 1999. Lei Nº 9.797, de 6 de maio de 1999. http://www.planalto.gov.br/ccivil_03/leis/L9797.htm. Dispõe sobre a cirurgia plástica reparadora da mama..

[3] BRASIL. 2023. Procedimentos Hospitalares do SUS - Por Local de Internação. Brasília, DF: Ministério da Saúde. https://datasus.saude.gov.br/

[4] J. S. Cardoso and M. J. Cardoso. 2007. Towards an Intelligent Medical System for the Aesthetic Evaluation of Breast Cancer Conservative Treatment. *Artif Intell Med* (2007). doi:10.1016/j.artmed.2007.02.007 Epub 2007 Apr 8. PMID: 17420117.

[5] M.J. Cardoso, J.S. Cardoso, H.P. Oliveira, and P. Gouveia. 2015. The Breast Cancer Conservative Treatment. Cosmetic Results - BCCT.core - Software for Objective Assessment of Esthetic Outcome in Breast Cancer Conservative Treatment: A Narrative Review. *Universidade do Porto. In Comput Methods Programs Biomed* (2015). doi:10.1016/j.cmpb.2015.11.010 Epub 2015 Dec 9. PMID: 26707372.

[6] E. C. Carvalho, A. M. Coelho, A. Conci, and M. F. O. Baffa. 2023. U-Net Convolutional Neural Networks for breast IR imaging segmentation on frontal and lateral view. *Computer Methods in Biomechanics and Biomedical Engineering: Imaging & Visualization* 11, 3 (2023), 311–316. doi:10.1080/21681163.2022.2040053

[7] A. Cozzi, G. Di Leo, N. Houssami, et al. 2025. Preoperative breast MRI reduces reoperations for unilateral invasive lobular carcinoma: a patient-matched analysis from the MIPA study. *European Radiology* (2025). doi:10.1007/s00330-024-11338-7

[8] Digit3D projects. 2023. *Digit3D projects.* http://www.ic.uff.br/aconci/pub2023 Acessado em 8 de novembro de 2023.

[9] Mahnaz Etehadtavakol, Mojtaba Sirati-Amsheh, Golnaz Moallem, and Eddie Yin Kwee Ng. 2025. Enhancing thyroid nodule classification: A comprehensive analysis of feature selection in thermography. *Infrared Physics Technology* 145 (2025), 105730. doi:10.1016/j.infrared.2025.105730

[10] G. Gallo, D. Allegra, Y. G. Atani, F. L. M. Milotta, F. Stanco, and G. Catanuto. 2016. Breast Shape Parametrization Through Planar Projections. In *Lecture Notes in Computer Science*. 135–146. doi:10.1007/978-3-319-48680-2_13

[11] M. Gezimati and G. Singh. 2025. Deep Learning for Multimodal Breast Cancer Characterization with Emergence of Terahertz and Infrared Imaging. *IEEE Transactions on Instrumentation and Measurement* (2025), 1–1. doi:10.1109/TIM.2025.3547084

[12] ISAPS. 2023. International Survey on Aesthetic/Cosmetic Procedures Performed in 2023. https://www.isaps.org

[13] D. Menezes, W. Fiorotti, L. Lima, E. Constantino, R. Leal, J. Landeiro, A. Conci, and M. Acioly. 2024. High-resolution intraoperative infrared thermography for the functional imaging and tumor resection maximization of a low-grade glioma: Technical case report. *Journal of Clinical Images and Medical Case Reports* 5 (2024), 5pp. doi:10.52768/2766-7820/2933 Open Access.

[14] E. Moura, G. Costa, T. Borchartt, and A.a Conci. 2024. A Tool for 3D Representation of the 2D Thermographic Breast Acquisitions. In *Nos Anais da 19ª Conferência Conjunta Internacional sobre Visão Computacional, Teoria e Aplicações de Imagens e Computação Gráfica - Volume 4: VISAPP*. SciTePress, 138–146. doi:10.5220/0012469500003660

[15] D.P. Navarro. 2017. *Desenvolvimento de um Sistema Computacional para Avaliação de Simetria Mamária.* Master's thesis. Universidade Positivo. https://repositorio.up.edu.br/jspui/handle/123456789/2260

[16] G. Novita, E. Millen, F. Zerwes, F. Pimentel, H. Oliveira Filho, and J. Pena Reis. 2025. *Tenho Doença de Paget da Mama, e agora?* https://www.cancerdemamabrasil.com.br/tenho-doenca-de-paget-da-mama-e-agora-cancer-de-mama/ Acessado em: 10 mar. 2025.

[17] R. Pacholczak, W. Klimek-Piotrowska, and P. Kuszmiersz. 2016. Associations of anthropometric measures on breast cancer risk in pre- and postmenopausal women–a case-control study. *Journal of Physiological Anthropology* 35 (3 2016), 7. doi:10.1186/s40101-016-0090-x

[18] N. Principigalli, A. E. L. S. Moura, and A. Conci. 2023. Could the Consideration of Symmetry be Statistically Significant for Breast Infrared Analysis?. In *Artificial Intelligence over Infrared Images for Medical Applications. AIIIMA 2023 (Lecture Notes in Computer Science, Vol. 14298)*, S.T. Kakileti, G. Manjunath, R.G. Schwartz, and A.F. Frangi (Eds.). Springer, Cham, 67–79. https://doi.org/10.1007/978-3-031-44511-8_5

[19] B. A. Sayed, A. S. Eldin, D. S. Elzanfaly, and A. S. Ghoneim. 2025. Breast Cancer Detection using Thermography and Convolutional Neural Networks (CNNs). In *Proceedings of the 11th International Conference on Advanced Intelligent Systems and Informatics (AISI 2025)*, A. E. Hassanien, R. Y. Rizk, A. Darwish, M. T. R. Alshurideh, V. Snášel, and M. F. Tolba (Eds.). Lecture Notes on Data Engineering and Communications Technologies, Vol. 238. Springer, Cham. doi:10.1007/978-3-031-81308-5_16

[20] L.F. Silva, D. C. M. Saade, G. O. Sequeiros, A. C. Silva, A. C. Paiva, R. S. Bravo, and A. Conci. 2014. A new database for mastology research with infrared image. *Journal of Medical Imaging and Health Informatics* 4, 1 (2014), 92–100. doi:10.1166/jmihi.2014.1226